DOI: 10.17344/acsi.2025.9406 *Acta Chim. Slov.* **2025,** *72,* 730–739

Scientific paper

Synthesis of Novel Indole Derivatives, Antiproliferative Activity, Apoptosis, and Molecular Docking Studies

Mahsa Toolabi[1,2], Zahra Sabzevari[2], Zakaria Forouzanfar[2], Ayyub Mojaddami[1,2,*]

[1] *Toxicology Research Center, Medical Basic Sciences Research Institute, Ahvaz Jundishapur University of Medical Sciences, Ahvaz, Iran.*

[2] *Department of Medicinal Chemistry, Faculty of Pharmacy, Ahvaz Jundishapur University of Medical Sciences, Ahvaz, Iran.*

** Corresponding author: E-mail: mojaddami.a@gmail.com*
Tel.: +98 61 33112278; Fax: +98 61 33738381

Received: 07-14-2025

Abstract

Novel indole-containing analogs were synthesized via a one-pot, multi-component Passerini reaction and subsequently evaluated for their anticancer activity against HeLa, MCF-7, and A549 cancer cell lines using the MTT assay. Among the synthesized compounds, (2-(cyclohexylamino)-1-(3-fluorophenyl)-2-oxoethyl 2-(1H-indol-3-yl)acetate (**4f**), which demonstrated the most potent cytotoxic activity, exhibited promising results with IC_{50} values of 17.71 and 19.92 μM against HeLa and MCF-7 cells, respectively. Flow cytometry analysis confirmed that compound **4f** significantly induced apoptosis in HeLa cells in a concentration-dependent manner. Furthermore, molecular docking studies into the active site of the anti-apoptotic protein Bcl-xL indicated that compound **4f** binds with good affinity, which is consistent with its considerable efficacy in the *in vitro* tests.

Keywords: Indole derivatives, Multi-component reaction (MCR), Antiproliferative activity, Bcl-xL inhibitors, Molecular docking study.

1. Introduction

Cancer has become the second leading cause of death worldwide, following cardiovascular diseases, according to World Health Organization (WHO) reports.[1] in 2020, over 19 million cases and 10 million deaths were recorded due to cancer.[2] Cancer is recognized as a major health problem with multifaceted and multimechanistic features. Although significant advances have been made in cancer diagnosis and management, successful cancer treatment remains a significant challenge. Limited efficacy and safety, as well as adverse toxicities, remain major issues with most current chemotherapeutic agents. Consequently, there is a growing demand for the discovery and development of new, safer anticancer agents.[3,4]

Indole core is a versatile bicyclic nitrogen-containing scaffold widely found in naturally occurring and synthetic bioactive structures.[5] Due to their unique physicochemical properties, biodiversity, and adaptability, indole-based derivatives have been extensively synthesized and evaluated for various pharmacological activities, including antimalarial[6], antibacterial[7,8], antifungal[9], anti-inflammatory[10] , antidepressant[11], antihypertensive[12], and antidiabetic effects.[13,14] Additionally, indole-containing compounds have been widely used as a core structure in the targeted design of anticancer agents.[15–18] Biological evaluations and mechanistic studies have revealed that anticancer indoles target diverse pathways in cancer cells, including tubulin polymerization, histone deacetylases (HDACs), Sirtuins, DNA topoisomerases, and anti-apoptotic proteins (such as Bcl-xL family). In this regard, numerous small molecules containing indole scaffolds as anticancer agents have been described and evaluated in recent years. These findings have led to the approval of several indole-based anticancer agents such as Panobinostat, Alectinib, Sunitinib, Osimertinib, Anlotinib, and Nintedanib for clinical use.[19,20]

Multi-component reactions (MCRs) have gained significant attention in organic synthesis as a novel, efficient, and valuable tool for preparing libraries of multifunctionalized compounds in a one-pot process. Due to

their high efficiency, low cost, and simple experimental procedures, MCRs have been widely utilized to synthesize various pharmaceutical and drug-like structures.[21] Among the most important MCRs, the Passerini three-component reaction, which involves the coupling of an aldehyde, a carboxylic acid, and an isocyanide to afford α-acyloxyamides, has recently attracted medicinal chemists for the synthesis of diverse multifunctional, biologically active compounds, including anticancer agents.[22]

Bcl-xL, a key anti-apoptotic regulator within the Bcl-2 family, is a well-established therapeutic target in oncology due to its central role in suppressing the intrinsic apoptotic pathway.[23] Its frequent overexpression in cancers promotes tumorigenesis and chemoresistance by sequestering pro-apoptotic proteins such as Bax and Bak, thereby preventing caspase activation.[24] Targeting Bcl-xL with novel therapeutics, such as small-molecule inhibitors that antagonize its interactions with proteins like Bax, represents a promising strategy to eliminate cancer cells by directly triggering their apoptotic machinery.

Building on these findings and our previous work in designing and synthesizing novel anticancer agents[25–28], several indole-based derivatives were synthesized via a one-pot, three-component Passerini reaction (Scheme 1). The target compounds were characterized and evaluated against three human carcinoma cell lines, including the cervical (HeLa), breast (MCF-7), and lung (A549), as well as against normal breast MCF-10A cells. Further molecular docking studies in the active site of the anti-apoptotic protein Bcl-xL and flow cytometry analysis were conducted to better understand the biological activities of the target compounds.

2. Results and Discussion

2. 1. Preparation of Novel Indole Derivatives

All new indole derivatives were synthesized via the three-component Passerini reaction using various benzaldehyde derivatives (**1**), cyclohexyl isocyanide (**2**), and

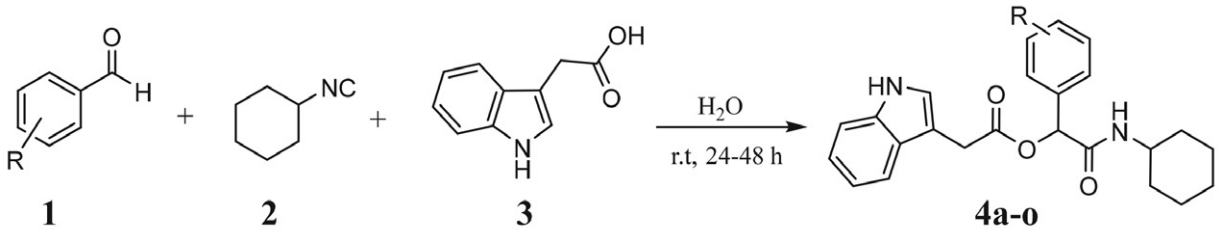

Scheme 1: Synthesis of target compounds (**4a-o**) through a three-component Passerini reaction. Reagents and conditions: benzaldehyde derivatives **1**, cyclohexyl isocyanide **2,** and indole-3-acetic acid **3**. distilled water, r.t., 24–48 h, 58–72%;

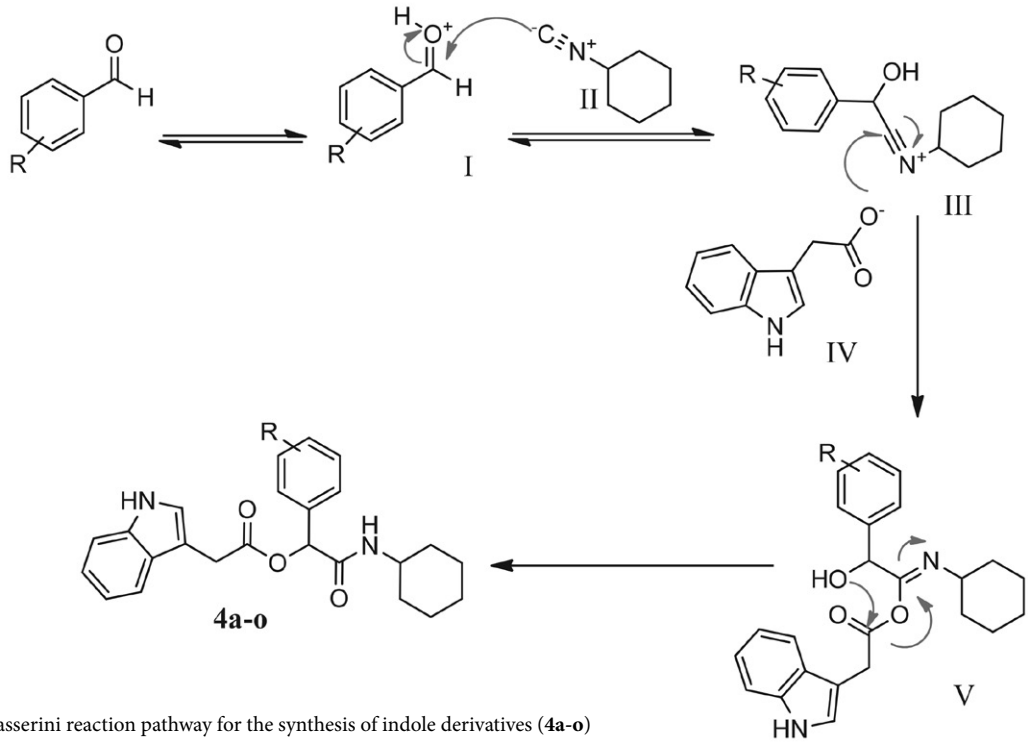

Scheme 2: Passerini reaction pathway for the synthesis of indole derivatives (**4a-o**)

indole-3-acetic acid (**3**) in a polar solvent, as shown in Scheme 1. The reaction was performed in a round-bottom flask by adding 1 mmol of each component in 5 mL of water as the solvent. The reaction mixture was then stirred at room temperature for 24 to 48 hours to obtain the target compounds in good yields (58–72%). In the first step, the carbonyl group of the benzaldehyde group was protonated (in the polar solvent. Subsequently, a nitrilium ion (was formed, followed by the addition of cyclohexyl isocyanide (*II*) to the protonated benzaldehyde derivatives. Upon addition of indole carboxylate (, an intermediate (was produced, which was converted to the final products (**4a-o**) through acyl transfer and amide tautomerization (Scheme 2).

2. 2. Antiproliferative Activity

MTT assay was used to evaluate the cytotoxic activities of the synthesized 2-(cyclohexylamino)-2-oxo-1-phenylethyl 2-(1H-indol-3-yl)acetate derivatives (**4a-o**), against three human cancer cell lines, including cervical (HeLa), breast (MCF-7), and lung (A549) cell lines as well as the normal MCF-10A cell line. The calculated IC_{50} values are summarized in Table 1, with Doxorubicin used as the reference drug. Based on the results obtained from the *in vitro* MTT assay, most of the synthesized compounds exhibited moderate antiproliferative activities compared to the reference drug, which showed the highest activity against HeLa cancer cells. The majority of compounds showed the lowest inhibitory activity against A549 cell line. Furthermore, the selectivity between cancer (MCF-7) and normal cell line (MCF-10A) was also determined. Most compounds showed no cytotoxicity against normal MCF-10A cells (IC_{50} = 100 μM). The selectivity index (SI), defined as the ratio of IC_{50} in normal human mammary epithelial cells (MCF-10A) to IC_{50} in breast cancer cells (MCF-7), was calculated to evaluate the selectivity of the compounds toward cancer cells.

The SI values for compound **4f** and Doxorubicin were **3.59** and **2.93**, respectively. These results indicate that compound **4f** has a higher selectivity index compared to Doxorubicin. Against the A549 cell line, most compounds exhibited moderate cytotoxicity (IC_{50} < 96 μM), with **4f** showing the highest potency (IC_{50} = 68.82 μM). Similarly, **4f** was the most active compound against MCF-7 cells (IC_{50}= 19.92 μM). For HeLa cells, the compounds displayed stronger overall activity, with **4f** again being the most potent (IC_{50}= 17.71 μM). Electron-donating groups (e.g., methyl, methoxy, and dimethoxy) consistently reduced activity across all cell lines.

Overall, the synthesized compounds showed the highest efficacy against HeLa cells, followed by MCF-7 and then A549 cell lines. The incorporation of electron-withdrawing groups at the *meta* position, particularly fluorine, yielded the most promising results. Compound **4f** emerged as the top performer, demonstrating potent and selective anticancer activity comparable to Doxorubicin (Table 1).

Table 1: IC_{50} values of compounds **4a-o** against HeLa, MCF-7, A549 and MCF-10A

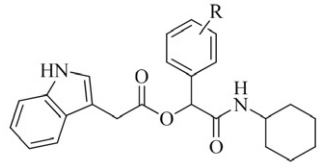

Compound	–R	IC_{50} (μM ± SEM)[a]			
		HeLa	MCF-7	A549	MCF-10A
4a	2-NO_2	71.90 ± 2.97	78.66 ± 1.69	89.61 ± 2.58	>100
4b	3-NO_2	30.77 ± 1.43	48.66 ± 2.17	>100	>100
4c	4-NO_2	43.89 ± 1.93	64.15 ± 2.37	>100	>100
4d	2,4-diNO_2	33.46 ± 2.28	51.18 ± 1.48	>100	>100
4e	2-F	62.34 ± 2.79	66.98 ± 1.51	96.48 ± 2.26	>100
4f	3-F	17.71 ± 0.95	19.92 ± 1.65	68.28 ± 1.89	71.45 ± 1.97
4g	4-F	35.44 ± 1.67	38.35 ± 1.25	90.85 ± 1.80	>100
4h	2-Cl	49.71 ± 2.81	85.14 ± 3.309	82.01 ± 2.82	>100
4i	3-Cl	27.84 ± 1.45	43.93 ± 1.26	86.83 ± 2.08	>100
4j	4-Cl	34.12 ± 1.41	41.59 ± 2.00	>100	>100
4k	2,4-diCl	58.75 ± 2.53	62.01 ± 1.78	79.08 ± 2.83	>100
4l	3-Br	43.29 ± 1.51	54.24 ± 1.37	77.12 ± 2.10	>100
4m	4-Me	55.55 ± 2.41	67.19 ± 1.59	>100	>100
4n	4-OMe	75.05 ± 1.32	62.12 ± 2.72	80.34 ± 1.79	>100
4o	3,4-diOMe	86.09 ± 1.85	> 100	91.69 ± 2.86	>100
Doxorubicin	–	11.64 ± 0.85	12.91 ± 0.61	9.38 ± 0.94	37.08 ± 1.82

[a] IC_{50} values were obtained from three separate experiments (n = 3) and expressed as means ± SEM.

The potent antiproliferative activity of compound **4f** – particularly against HeLa and MCF-7 cells – prompted further investigation into its mechanism of action, including apoptosis induction and molecular docking studies (discussed in Sections 2.3 and 2.4). Notably, the structure-activity relationship (SAR) analysis revealed that electron-withdrawing groups (e.g., F, Cl, and Br) significantly enhanced activity, with *meta*-substitution being particularly favorable. These findings underscore the potential of compound **4f** as a lead compound for further development.

2. 3. Apoptosis-inducing Activity

To investigate the potential mechanism of anti-cancer activity of the most potent compound **4f** against HeLa cancer cells, flow-cytometry analysis was performed using Annexin V-FITC/propidium iodide (Annexin V/PI) double-staining assay. HeLa cells were treated with varying concentrations of compound **4f** (10–30 μM) for 24 hours, with untreated HeLa cells serving as the negative control. The total apoptotic cell population was defined as the sum of early apoptosis (Annexin V+/PI-) and late apoptosis (Annexin V+/PI+). In untreated cells, only 5.82% were in the apoptotic stage. Treatment with compound **4f** at 10 μM resulted in 16.6% apoptosis and 0.7% necrosis (Fig. 1). Higher concentrations of 20 and 30 μM induced stronger apoptotic responses, with 26.94% and 34.66% apoptosis, respectively. These results confirm that compound **4f** induces apoptosis in HeLa cancer cells in a dose-dependent manner.

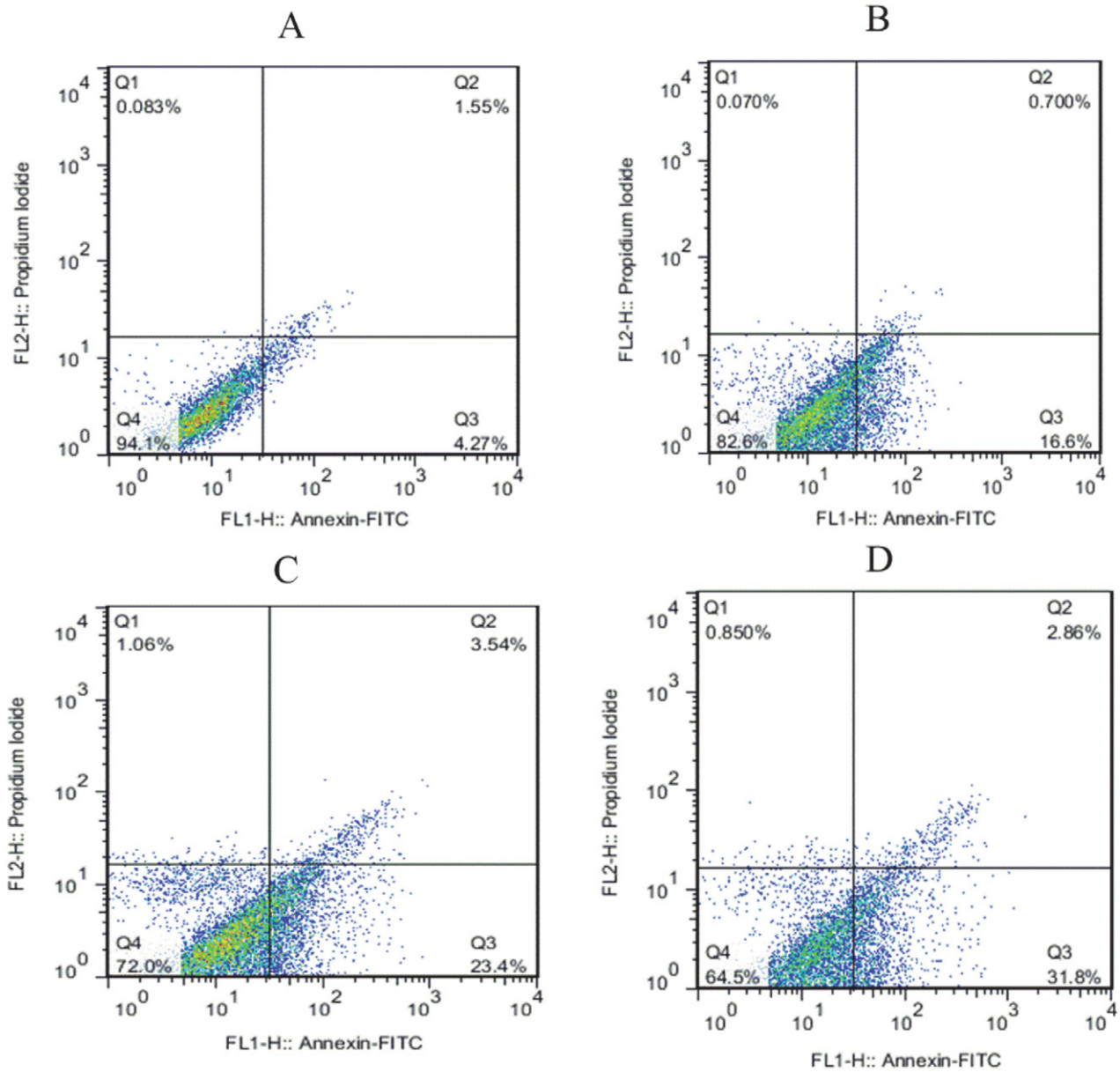

Figure 1. Flow cytometry analysis of HeLa cells treated with compound **4f** (A) Untreated negative control group; :(B) treated with **4f** at 10 μM concentration; (C) treated with **4f** at 20 μM concentration. (D) treated with **4f** at 30 μM concentration.

2. 4. Molecular Docking Results

A molecular docking study was applied to investigate ligand–protein interactions and estimate ligand-binding affinity between the synthesized indole derivatives (**4a–o**) in the active site of anti-apoptotic protein Bcl-xL (PDB code: 4C5D) using AutoDock 4.2 software. The binding free energies (ΔG_b, kcal/mol) and hydrogen bond interactions obtained from the docking studies are shown in Table 2. The lowest binding energies among the synthesized compounds belongs to compounds **4l** and **4h**, with values of –10.60 and –10.59 kcal/mol, respectively. The most potent compound from *in vitro* assays showed a low binding energy of –9.97 kcal/mol. The results confirmed stable interactions between the studied compounds and the active site of Bcl-xL.

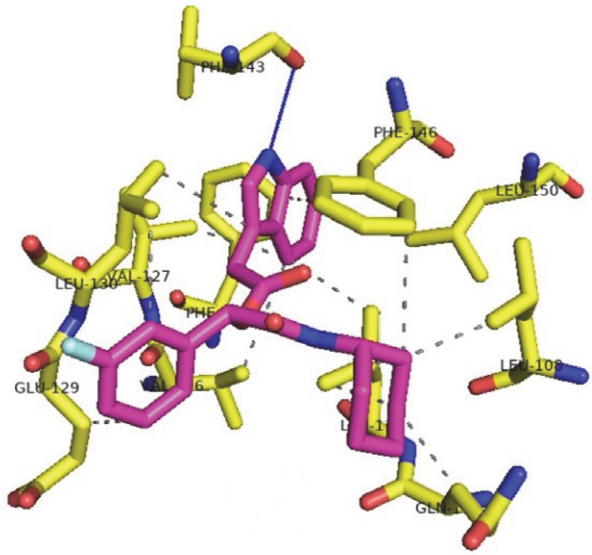

Figure 2: The binding model of compound **4f** to Bcl-xL protein by PyMOL.

Table 2: Free binding energy (kcal/mol) of synthesized compounds

Compound	Binding energy (ΔG_b, kcal/mol)	H-bond Interactions
4a	–10.13	Arg139, Leu130, Phe143
4b	–10.06	Val127, Arg139, Ala104
4c	–9.80	Glu129, Arg139, Phe143
4d	–9.66	Val127, Phe143
4e	–9.97	Val127, Phe143
4f	–9.97	Val127, Phe143, Val126
4g	–9.87	Val127, Phe143
4h	–10.59	Val127, Phe143
4i	–10.57	Val127, Phe143
4j	–10.42	Val127, Phe143
4k	–10.39	Glu129, Phe143
4l	–10.60	Val127, Leu130, Phe143
4m	–10.26	Val127, Gln111
4n	–10.27	Val127, Phe143, Gln111, Val126
4o	–10.05	Val127, Phe143, Val126
Cocrystal ligand	–10.87	Phe143, Arg139, Leu130

The amino acids involved in hydrogen bonds between the ligand and the protein are listed in Table 2. It is clear that the amino acids Val127 and Phe143 of Bcl-xL have the strongest interactions with different ligands and play a key role in receptor–ligand binding. As a result, the compound **4f** formed key interactions in the active site of the Bcl-xL protein with residues Phe143 and Arg139, as well as a π–alkyl interaction between the indole core of **4f**

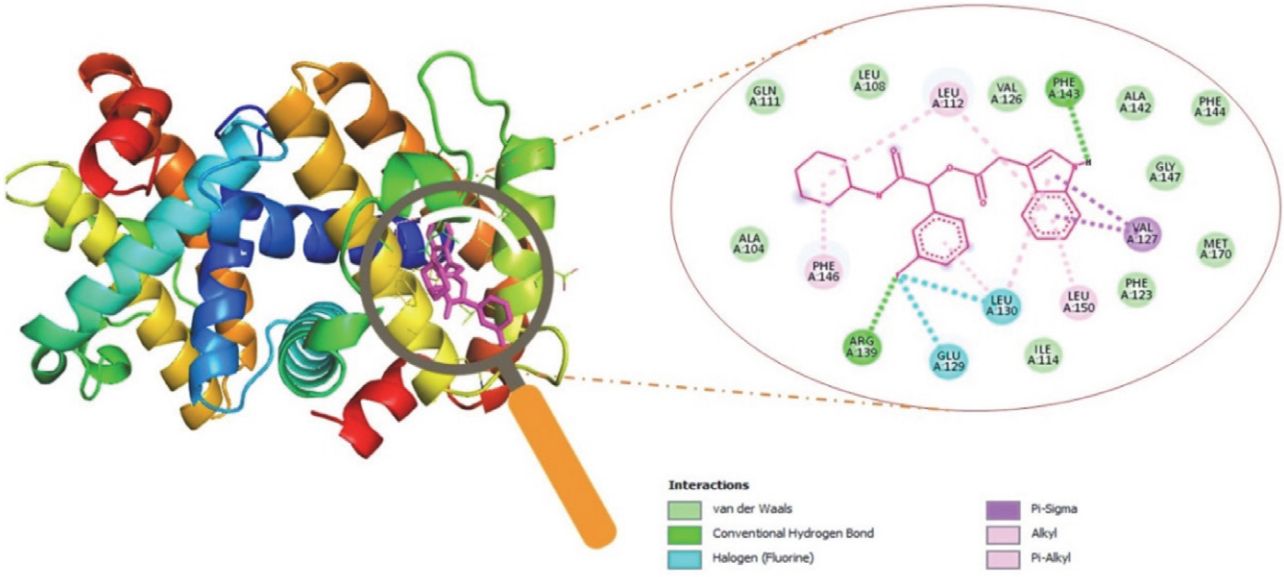

Figure 3: Three-dimensional and two-dimensional interaction of the **4f** compound with the Bcl-xL protein by PyMOL and Discovery Studio Visualizer 3.0.

and Val126 (Fig. 2 and Fig. 3). The results confirmed that **4f** fitted well into the active site of Bcl-xL through strong hydrogen bonds and π–alkyl interactions with a binding energy of –9.97 kcal/mol.

3. Conclusion

A series of indole-based derivatives were synthesized via a one-pot, multi-component Passerini reaction and evaluated for anti-cancer activity using MTT assays against HeLa (cervical), MCF-7 (breast), and A549 (lung) cancer cell lines. Notably, the 3-F substituted derivative **4f** effectively inhibited proliferation in HeLa and MCF-7 cells (IC_{50} = 17.71 and 19.92 μM, respectively) and dose-dependently induced apoptosis in HeLa cells. Molecular docking revealed strong interactions of **4f** with the Bcl-xL protein, exhibiting low binding energies and key hydrogen and noncovalent bonds. This study establishes a foundation for lead identification, with compounds showing moderate micromolar potencies suitable for further optimization. Future work could include additional assays and molecular dynamics simulations to deepen insights into ligand–protein stability.

4. Experimental

4. 1. Materials and Methods

Reagents and solvents were purchased from commercial sources, Merck and Sigma Aldrich companies, and used without further purification. Low-resolution mass spectra were obtained on an Agilent mass spectrometer. A Perkin-Elmer 1600 FT-IR spectrophotometer was used to record FTIR spectra on KBr disks (V_{max} in cm^{-1}). Melting points were determined on the WRS-1A digital melting point. The reaction progress was imaged by thin layer chromatography (TLC) using ultraviolet 254 nm. Spectra ^{1}H NMR and ^{13}C NMR were recorded on the Varian-INOVA 500 MHz and 300 MHz spectrometer. Chemical shifts were reported in ppm in $CDCl_3$ or DMSO relative to tetramethylsilane (TMS) as the internal standard. The signals were abbreviated as s, singlet; d, doublet; t, triplet, and m, multiplet, and coupling constants have been reported (J) in Hertz (Hz). Elemental analyses were performed using a Perkin-Elmer 240-C apparatus (Perkin-Elmer, Beaconsfield, UK) and were within ± 0.4% of the theoretical values for C, H, and N.

4. 2. General procedure for the synthesis of indole derivatives by Paserini method: 4a-o.

Effective indole derivatives were synthesized through a three-component Passerini reaction, as shown in Scheme 1. In a reaction vessel, 1 mmol of 3-acetic acid indole was stirred in 6 mL of distilled water for 10 minutes. Then, 1 mmol of the corresponding benzaldehyde derivative and 1 mmol of cyclohexyl isocyanide were added, and the mixture was continuously stirred for 24–48 hours. The resulting precipitate was filtered, washed with water, and recrystallized from methanol. All final compounds submitted for biological testing were of high purity, confirmed to be ≥ 95% by elemental (CHN) analysis.[29]

2-(cyclohexylamino)-1-(2-nitrophenyl)-2-oxoethyl 2-(1H-indol-3-yl)acetate (4a)

Yellow solid; yield: 68%; mp: 123–125 ; IR (KBr; cm^{-1}): 3263 (N–H), 3142 (CON–H), 1715 (C=O, ester), 1671 (C=O, amide), 1523 (N–O), 1344 (N–O). ^{1}H NMR (500 MHz, DMSO-d_6) δ: 10.98 (s, 1H), 8.03 (d, *J* = 8.1 Hz, 1H), 7.99 (d, *J* = 8.0 Hz, 1H), 7.67 (t, *J* = 7.6 Hz, 1H), 7.60 (t, *J* = 7.8 Hz, 1H), 7.52–7.49 (m, 2H), 7.37 (d, *J* = 8.2 Hz, 1H), 7.31 (s, 1H), 7.09 (t, *J* = 7.6 Hz, 1H), 6.98 (t, *J* = 7.5 Hz, 1H), 6.54 (s, 1H), 3.91 (s, 2H), 3.56–3.50 (m, 1H), 1.69–1.61 (m, 4H), 1.5–1.52 (m, 1H), 1.24–1.18 (m, 2H), 1.1–1.06 (m, 3H). ^{13}CNMR (125 MHz, DMSO-d_6) δ: 170.9, 165.8, 148.9, 136.5, 134.0, 130.9, 130.2, 129.2, 127.5, 125.1, 124.7 (2C), 121.6, 119.0 (2C), 111.9, 106.8, 70.9, 48.4, 32.4, 30.8, 25.5, 24.9, 24.8. Anal. Calcd. For $C_{24}H_{25}N_3O_5$: C, 66.19; H, 5.79; N, 9.65. Found: C, 66.41; H, 5.51; N, 9.49; ESI-MS *m/z*: 435.6 M^+.

2-(Cyclohexylamino)-1-(3-nitrophenyl)-2-oxoethyl 2-(1H-indol-3-yl)acetate (4b)

Yellow solid; yield: 66%; mp: 15-156 ; IR (KBr; cm^{-1}): 3329 (N–H), 3258 (CON–H), 1710 (C=O, ester), 1655 (C=O, amide), 1531 (N–O), 1352 (N–O). ^{1}H NMR (500 MHz, DMSO-d_6) δ: 10.96 (s, 1H), 8.32 (s, 1H), 8.20 (d, *J* = 8.2 Hz, 1H), 8.14 (d, *J* = 7.9 Hz, 1H), 7.89 (d, *J* = 7.7 Hz, 1H), 7.67 (t, *J* = 8.0 Hz, 1H), 7.51 (d, *J* = 7.9 Hz, 1H), 7.35 (d, *J* = 8.0 Hz, 1H), 7.30 (s, 1H), 7.07 (t, *J* = 7.6 Hz, 1H), 6.95 (t, *J* = 7.4 Hz, 1H), 6.01 (s, 1H), 3.91 (s, 2H), 3.50–3.44 (m, 1H), 1.70–1.63 (m, 2H), 1.61–1.52 (m, 3H), 1.2–1.17 (m, 3H), 1.14–1.06 (m, 2H). ^{13}C NMR (125 MHz, DMSO-d_6) δ: 171.0, 166.5, 148.1, 138.6, 136.5, 134.0, 130.5, 127.4, 124.7, 123.8, 122.1 (2C), 121.5, 119.0, 118.9, 111.8, 106.9, 74.4, 48.1, 32.3, 30.9, 25.5, 24.8, 24.7. Anal. Calcd. For $C_{24}H_{25}N_3O_5$: C, 66.19; H, 5.79; N, 9.65. Found: C, 66.21; H, 5.82; N, 9.51; ESI-MS *m/z*: 435.5 M^+.

2-(Cyclohexylamino)-1-(4-nitrophenyl)-2-oxoethyl 2-(1H-indol-3-yl)acetate (4c)

Yellow solid; yield: 69%; mp: 144–146 ; IR (KBr; cm^{-1}): 3398 (N–H), 3309 (CON–H), 1742 (C=O, ester), 1673 (C=O, amide), 1521 (N–O), 1351 (N–O). ^{1}H NMR (500 MHz, DMSO-d_6) δ: 10.97 (s, 1H), 8.22 (d, *J* = 6.9 Hz, 2H), 8.12 (d, *J* = 7.8 Hz, 1H), 7.73 (d, *J* = 6.9 Hz, 2H), 7.52 (d, *J* = 8.1 Hz, 1H), 7.36 (d, *J* = 8.1 Hz, 1H), 7.31 (s, 1H), 7.08 (t, *J* = 7.5 Hz, 1H), 6.97 (t, *J* = 7.6 Hz, 1H), 6.02 (s, 1H), 3.92 (s, 2H), 3.49–3.43 (m, 1H), 1.71–1.63 (m, 2H), 1.59–1.49 (m, 3H), 1.21–1.12 (m, 4H), 1.10–1.01 (m, 1H). ^{13}C NMR

(125 MHz, DMSO-d_6) δ: 171.0, 166.3, 147.8, 143.7, 136.5, 128.6 (2C), 127.5, 124.7, 123.9 (2C), 121.6, 119.0, 118.9, 111.9, 110.3, 106.9, 74.6, 48.1, 32.3, 30.9, 25.5, 24.8, 24.7. Anal. Calcd. For $C_{24}H_{25}N_3O_5$: C, 66.19; H, 5.79; N, 9.65. Found: C, 66.31; H, 5.67; N, 9.45; ESI-MS *m/z*: 435.5 M^+.

2-(Cyclohexylamino)-1-(2,4-dinitrophenyl)-2-oxoethyl 2-(1H-indol-3-yl)acetate (4d)

Yellow solid; yield: 61%; mp: 167–169 ; IR (KBr; cm^{-1}): 3310 (N–H), 3251 (CON–H), 1748 (C=O, ester), 1666 (C=O, amide), 1525 (N–O), 1374 (N–O). ^{1}H NMR (500 MHz, DMSO-d_6) δ: 10.99 (s, 1H), 8.72 (s, 1H), 8.41 (d, *J* = 8.4 Hz, 1H), 8.13 (d, *J* = 7.9 Hz, 1H), 7.74 (d, *J* = 8.6 Hz, 1H), 7.50 (d, *J* = 8.0 Hz, 1H), 7.37 (d, *J* = 8.1 Hz, 1H), 7.31 (s, 1H), 7.08 (t, *J* = 7.6 Hz, 1H), 6.97 (t, *J* = 7.5 Hz, 1H), 6.63 (s, 1H), 3.96 (s, 2H), 3.55–3.51 (m, 1H), 1.70–1.59 (m, 4H), 1.55–1.52 (m, 1H), 1.27–1.18 (m, 2H), 1.16–1.10 (m, 3H). ^{13}CNMR (125 MHz, DMSO-d_6) δ: 170.8, 164.9, 148.6, 147.8, 137.3, 136.5, 130.6, 128.0, 127.4, 124.8 (2C), 121.6, 120.5, 119.0, 118.9, 111.9, 106.6, 70.7, 48.6, 32.3, 30.8, 25.5, 24.9, 24.8. Anal. Calcd. For $C_{24}H_{24}N_4O_7$: C, 60.00; H, 5.03; N, 11.66. Found: C, 60.12; H, 5.25; N, 11.47; ESI-MS *m/z*: 480.7 M^+.

2-(Cyclohexylamino)-1-(2-fluorophenyl)-2-oxoethyl 2-(1H-indol-3-yl)acetate (4e)

White solid; yield: 59%; mp: 122–124 ; IR (KBr; cm^{-1}): 3381 (N–H), 3224 (CON–H), 1741 (C=O, ester), 1662 (C=O, amide), 1519, 1225. ^{1}H NMR (500 MHz, DMSO-d_6) δ: 10.96 (s, 1H), 7.84 (d, *J* = 7.9 Hz, 1H), 7.49 (d, *J* = 7.9 Hz, 1H), 7.46-7.37 (m, 2H), 7.35 (d, *J* = 8.0 Hz, 1H), 7.28 (s, 1H), 7.26-7.17 (m, 2H), 7.08 (t, *J* = 7.6 Hz, 1H), 6.96 (t, *J* = 7.5 Hz, 1H), 6.12 (s, 1H), 3.90–3.82 (m, 2H), 3.56–3.50 (m, 1H), 1.68–1.59 (m, 4H), 1.54–1.51 (m, 1H), 1.23–1.12 (m, 2H), 1.10–1.01 (m, 3H). ^{13}C NMR (125 MHz, DMSO-d_6) δ: 171.0, 166.2, 161.6 (d, *J* = 246.4 Hz), 136.5, 131.4 (d, *J* = 8.0 Hz), 129.8 (d, *J* = 3.3 Hz), 127.4, 125.0, 124.9, 124.6, 123.8 (d, *J* = 13.9 Hz), 121.5, 118.9 (2C), 116.0 (d, *J* = 21.1 Hz), 111.8, 107.0, 69.4, 48.1, 32.3, 30.9, 25.5, 25.0, 24.9. Anal. Calcd. For $C_{24}H_{25}FN_2O_3$: C, 70.57; H, 6.17; N, 6.86. Found: C, 70.41; H, 6.32; N, 6.69; ESI-MS *m/z*: 408.6 M^+.

2-(Cyclohexylamino)-1-(3-fluorophenyl)-2-oxoethyl 2-(1H-indol-3-yl)acetate (4f)

White solid; yield: 58%; mp: 126–128 ; IR (KBr; cm^{-1}): 3322 (N–H), 3257 (CON–H), 1709 (C=O, ester), 1653 (C=O, amide). ^{1}H NMR (300 MHz, DMSO-d_6) δ: 10.97 (s, 1H), 7.99 (d, J = 7.9 Hz, 1H), 7.53 (d, *J* = 7.8 Hz, 1H), 7.44–7.35 (m, 2H), 7.31–7.24 (m, 3H), 7.17 (t, *J* = 8.5 Hz, 1H), 7.08 (t, *J* = 7.6 Hz, 1H), 6.97 (t, *J* = 7.4 Hz, 1H), 5.88 (s, 1H), 3.90 (s, 2H), 3.52–3.42 (m, 1H), 1.71–1.61 (m, 2H), 1.56–1.52 (m, 3H), 1.28–1.12 (m, 3H), 1.10–0.95 (m, 2H). ^{13}C NMR (75 MHz, DMSO-d_6) δ: 170.6, 166.4, 162.5 (d, *J* = 242.4 Hz), 138.7 (d, *J* = 7.7 Hz), 136.1, 130.4 (d, *J* = 8.3 Hz), 127.0, 124.2, 123.2, 123.1, 121.1, 118.6, 118.5, 115.2 (d, *J* = 21.0 Hz), 113.8 (d, *J* = 22.8 Hz), 111.4, 106.6, 74.3, 47.6, 31.9, 30.5, 25.1, 24.4, 24.4. Anal. Calcd. For $C_{24}H_{25}FN_2O_3$: C, 70.57; H, 6.17; N, 6.86. Found: C, 70.69; H, 6.24; N, 6.49; ESI-MS *m/z*: 408.4 M^+.

2-(Cyclohexylamino)-1-(4-fluorophenyl)-2-oxoethyl 2-(1H-indol-3-yl)acetate (4g)

White solid; yield: 65%; mp: 152–154 ; IR (KBr; cm^{-1}): 3314 (N–H), 3225 (CON–H), 1715 (C=O, ester), 1653 (C=O, amide). ^{1}H NMR (300 MHz, DMSO-d_6) δ: 10.96 (s, 1H), 7.92 (d, *J* = 7.8 Hz, 1H), 7.55–7.41 (m, 3H), 7.35 (d, *J* = 8.1 Hz, 1H), 7.30–7.28 (m, 1H), 7.19 (t, *J* = 8.9 Hz, 2H), 7.08 (t, *J* = 7.5 Hz, 1H), 6.96 (t, *J* = 7.4 Hz, 1H), 5.85 (s, 1H), 3.86 (s, 2H), 3.51–3.41 (m, 1H), 1.70–1.61 (m, 2H), 1.54–1.50 (m, 3H), 1.23–1.04 (m, 4H), 1.01–0.92 (m, 1H). ^{13}C NMR (75 MHz, DMSO-d_6) δ: 170.6, 166.7, 162.5 (d, *J* = 243.1 Hz), 136.0, 132.3, 132.3, 129.4, 129.3, 127.0, 124.2, 121.1, 118.5 (d, *J* = 8.5 Hz), 115.2 (d, *J* = 2 Hz), 111.4, 106.6, 74.3, 47.5, 31.9, 30.5, 25.0, 24.4, 24.4. Anal. Calcd. For $C_{24}H_{25}FN_2O_3$: C, 70.57; H, 6.17; N, 6.86. Found: C, 70.69; H, 6.01; N, 6.95; ESI-MS *m/z*: 408.1 M^+.

1-(2-Chlorophenyl)-2-(cyclohexylamino)-2-oxoethyl 2-(1H-indol-3-yl)acetate (4h)

White solid; yield: 66%; mp: 133–135 ; IR (KBr; cm^{-1}): 3382 (N–H), 3281 (CON–H), 1745 (C=O, ester), 1665 (C=O, amide), 1530. ^{1}H NMR (500 MHz, DMSO-d_6) δ: 10.96 (s, 1H), 7.95 (d, *J* = 8.0 Hz, 1H), 7.49 (d, *J* = 7.9 Hz, 2H), 7.40–7.32 (m, 4H), 7.28 (s, 1H), 7.08 (t, *J* = 7.6 Hz, 1H), 6.96 (t, *J* = 7.4 Hz, 1H), 6.20 (s, 1H), 3.90–3.82 (m, 2H), 3.58–3.52 (m, 1H), 1.71–1.60 (m, 4H), 1.54–1.52 (m, 1H), 1.24–1.19 (m, 2H), 1.14–1.04 (m, 3H). ^{13}C NMR (125 MHz, DMSO-d_6) δ: 171.0, 166.1, 136.5, 134.2, 133.9, 130.9, 130.0, 129.8, 127.8, 127.4, 124.7 (2C), 121.5, 119.0, 118.9, 111.8, 107.0, 72.4, 48.2, 32.4, 30.8, 25.5, 25.0, 24.9. Anal. Calcd. For $C_{24}H_{25}ClN_2O_3$: C, 67.84; H, 5.93; N, 6.59. Found: C, 67.99; H, 5.79; N, 6.45; ESI-MS *m/z*: 424.1 M^+.

1-(3-Chlorophenyl)-2-(cyclohexylamino)-2-oxoethyl 2-(1H-indol-3-yl)acetate (4i)

White solid; yield: 62%; mp: 113–115 ; IR (KBr; cm^{-1}): 3325 (N–H), 3274 (CON–H), 1711 (C=O, ester), 1656 (C=O, amide), 1571, 1241.60. ^{1}H NMR (300 MHz, DMSO-d_6) δ: 10.97 (s, 1H), 8.01 (d, *J* = 7.8 Hz, 1H), 7.54–7.51 (m, 2H), 7.50–7.30 (m, 5H), 7.08 (t, *J* = 7.5 Hz, 1H), 6.97 (t, *J* = 7.4 Hz, 1H), 5.86 (s, 1H), 3.89 (s, 2H), 3.52–3.42 (m, 1H), 1.70–1.62 (m, 2H), 1.56–1.52 (m, 3H), 1.24–1.14 (m, 3H), 1.10–1.00 (m, 2H). ^{13}C NMR (75 MHz, DMSO-d_6) δ: 170.6, 166.4, 138.4, 136.1, 133.0, 130.3, 128.4, 127.0, 126.9, 126.8, 125.7, 124.2, 121.1, 118.6, 118.5, 111.4, 106.6, 74.3, 47.6, 32.1, 31.9, 30.5, 24.5, 24.4. Anal. Calcd. For $C_{24}H_{25}ClN_2O_3$: C, 67.84; H, 5.93; N, 6.59. Found: C, 67.68; H, 5.84; N, 6.73; ESI-MS *m/z*: 424.5 M^+.

1-(4-Chlorophenyl)-2-(cyclohexylamino)-2-oxoethyl 2-(1H-indol-3-yl)acetate (4j)

White solid; yield: 65%; mp: 152–154; IR (KBr; cm^{-1}):

3356 (N–H), 3239 (CON–H), 1712 (C=O, ester), 1648 (C=O, amide). ^{1}H NMR (500 MHz, DMSO-d_6) δ: 10.96 (s, 1H), 7.95 (d, *J* = 7.9 Hz, 1H), 7.51 (d, *J* = 7.9 Hz, 1H), 7.47 (d, *J* = 8.5 Hz, 2H), 7.43 (d, *J* = 8.5 Hz, 2H), 7.35 (d, *J* = 8.0 Hz, 1H), 7.32–7.26 (m, 1H), 7.08 (t, *J* = 7.6 Hz, 1H), 6.97 (t, *J* = 7.4 Hz, 1H), 5.85 (s, 1H), 3.87 (s, 2H), 3.49–3.43 (m, 1H), 1.69–1.62 (m, 2H), 1.59–1.49 (m, 3H), 1.23–1.17 (m, 2H), 1.14–1.11 (m, 2H), 1.09–1.01 (m, 1H). ^{13}C NMR (125 MHz, DMSO-d_6) δ: 171.1, 167.0, 136.5, 135.5, 133.5, 129.4, 128.8, 127.5, 124.6, 121.5, 119.0, 118.9, 111.8, 110.3, 107.0, 74.7, 48.0, 32.4, 31.0, 25.5, 24.8, 24.8. MS m/z (%): 423.3 M^+ (0.44), 157.1 (60.28), 130.1 (74.37), 43.1 (100). Anal. Calcd. For $C_{24}H_{25}ClN_2O_3$: C, 67.84; H, 5.93; N, 6.59. Found: C, 67.94; H, 5.62; N, 6.69; ESI-MS *m/z*: 424.2 M^+.

2-(Cyclohexylamino)-1-(2,4-dichlorophenyl)-2-oxoethyl 2-(1H-indol-3-yl)acetate (4k)

White solid; yield: 60%; mp: 121–123 ; IR (KBr; cm^{-1}): 3386 (N–H), 3284 (CON–H), 1746 (C=O, ester), 1664 (C=O, amide), 1532.52. ^{1}H NMR (500 MHz, DMSO-d_6) δ: 10.96 (s, 1H), 8.01 (d, *J* = 8.0 Hz, 1H), 7.66 (s, 1H), 7.48 (d, *J* = 8.0 Hz, 1H), 7.45–7.40 (m, 1H), 7.40–7.33 (m, 2H), 7.28 (s, 1H), 7.08 (t, *J* = 7.6 Hz, 1H), 6.96 (t, *J* = 7.4 Hz, 1H), 6.16 (s, 1H), 3.86 (s, 2H), 3.58–3.52 (m, 1H), 1.71–1.60 (m, 4H), 1.54–1.52 (m, 1H), 1.27–1.18 (m, 2H), 1.17–1.05 (m, 3H). ^{13}C NMR (125 MHz, DMSO-d_6) δ: 170.9, 165.8, 136.5, 134.8, 134.6, 133.5, 131.1, 129.5, 128.0, 127.5, 124.7 (2C), 121.6, 118.9 (2C), 111.8, 106.9, 71.9, 48.3, 32.4, 30.8, 25.5, 25.0, 24.9. Anal. Calcd. For $C_{24}H_{24}Cl_2N_2O_3$: C, 62.75; H, 5.27; N, 6.10. Found: C, 62.59; H, 5.48; N, 6.27; ESI-MS *m/z*: 458.2 M^+.

1-(3-Bromophenyl)-2-(cyclohexylamino)-2-oxoethyl 2-(1H-indol-3-yl)acetate (4l)

White solid; yield: 63%; mp: 108–110 ; IR (KBr; cm^{-1}): 3328 (N–H), 3262 (CON–H), 1712 (C=O, ester), 1657 (C=O, amide), 1530. ^{1}H NMR (500 MHz, DMSO-d_6) δ: 10.96 (s, 1H), 7.99 (d, *J* = 7.9 Hz, 1H), 7.63 (s, 1H), 7.53 (t, *J* = 7.2 Hz, 2H), 7.45 (d, *J* = 7.7 Hz, 1H), 7.36–7.29 (m, 3H), 7.08 (t, *J* = 7.6 Hz, 1H), 6.97 (t, *J* = 7.4 Hz, 1H), 5.84 (s, 1H), 3.89 (s, 2H), 3.50–3.43 (m, 1H), 1.69–1.57 (m, 2H), 1.52–1.50 (m, 3H), 1.25–1.17 (m, 3H), 1.14–0.99 (m, 2H). ^{13}C NMR (125 MHz, DMSO-d_6) δ: 171.0, 166.8, 139.0, 136.5, 131.7, 131.0, 130.1, 127.5, 126.5, 124.6 (2C), 121.9, 121.5, 119.0, 118.9, 111.8, 107.0, 74.7, 48.0, 32.4, 30.9, 25.5, 24.9, 24.8. Anal. Calcd. For $C_{24}H_{25}BrN_2O_3$: C, 62.75; H, 5.27; N, 6.10. Found: C, 62.91; H, 5.12; N, 6.34; ESI-MS *m/z*: 468.3 M^+.

2-(Cyclohexylamino)-2-oxo-1-(p-tolyl)ethyl 2-(1H-indol-3-yl)acetate (4m)

White solid; yield: 60%; mp: 141–143 ; IR (KBr; cm^{-1}): 3325 (N–H), 3245 (CON–H), 1654 (C=O, amide), 1566, 1243. ^{1}H NMR (300 MHz, DMSO-d_6) δ: 10.96 (s, 1H), 7.83 (d, *J* = 7.9 Hz, 1H), 7.51 (d, *J* = 7.8 Hz, 1H), 7.37–7.29 (m, 4H), 7.15 (d, *J* = 7.9 Hz, 2H), 7.08 (t, *J* = 7.6 Hz, 1H), 6.96 (t, *J* = 7.4 Hz, 1H), 5.80 (s, 1H), 3.85 (s, 2H), 3.52–3.41 (m, 1H), 2.28 (s, 3H), 1.69–1.61 (m, 4H), 1.54–1.49 (m, 1H), 1.29–1.12 (m, 3H), 1.07–0.91 (m, 2H). ^{13}C NMR (75 MHz, DMSO-d_6) δ: 170.7, 167.0, 137.8, 136.1, 133.1, 128.9 (2C), 127.2 (2C), 127.0, 124.2 (2C), 121.15, 118.6, 118.5, 111.4, 106.7, 75.0, 47.5, 32.0, 30.6, 25.1, 24.5, 24.4, 20.7. Anal. Calcd. For $C_{25}H_{28}N_2O_3$: C, 74.23; H, 6.98; N, 6.93. Found: C, 74.39; H, 6.75; N, 6.82; ESI-MS *m/z*: 404.3 M^+.

2-(Cyclohexylamino)-1-(4-methoxyphenyl)-2-oxoethyl 2-(1H-indol-3-yl)acetate (4n)

White solid; yield: 72%; mp: 132–134 ; IR (KBr; cm^{-1}): 3319 (N–H), 3251 (CON–H), 1700 (C=O, ester), 1649 (C=O, amide), 1249 (C–O, ether). ^{1}H NMR (500 MHz, DMSO-d_6) δ: 10.95 (s, 1H), 7.80 (d, *J* = 8.0 Hz, 1H), 7.51 (d, *J* = 7.9 Hz, 1H), 7.39–7.35 (m, 3H), 7.29 (s, 1H), 7.08 (t, *J* = 7.6 Hz, 1H), 6.97 (t, *J* = 7.5 Hz, 1H), 6.92 (d, *J* = 6.9 Hz, 2H), 5.79 (s, 1H), 3.85–3.81 (m, 2H), 3.74 (s, 3H), 3.50–3.46 (m, 1H), 1.70–1.59 (m, 2H), 1.56–1.52 (m, 3H), 1.25–1.11 (m, 4H), 1.09–0.97 (m, 1H). ^{13}C NMR (125 MHz, DMSO-d_6) δ: 171.2, 167.5, 159.8, 136.5, 129.2 (2C), 128.5, 127.5, 124.6 (2C), 121.5, 119.0, 118.9, 114.1 (2C), 111.8, 107.2, 75.2, 55.5, 47.9, 32.4, 31.0, 25.5, 24.9, 24.8. MS m/z (%): 420.5 M^+ (2.17), 247.3 (61.39), 157.1 (25.16), 130.2 (100), 98.2 (25.31), 77.1 (13.04), 55.1 (14.79). Anal. Calcd. For $C_{25}H_{28}N_2O_4$: C, 71.19; H, 6.47; N, 6.91. Found: C, 71.41; H, 6.71; N, 6.66; ESI-MS *m/z*: 420.5 M^+.

2-(Cyclohexylamino)-1-(3,4-dimethoxyphenyl)-2-oxoethyl 2-(1H-indol-3-yl)acetate (4o)

White solid; yield: 68%; mp: 160–162 decomp; IR (KBr; cm^{-1}): 3386 (N–H), 3325 (CON–H), 1738 (C=O, ester), 1667 (C=O, amide), 1246 (C–O, ether), 1131. ^{1}H NMR (500 MHz, DMSO-d_6) δ: 10.96 (s, 1H), 7.80 (d, *J* = 8.0 Hz, 1H), 7.54 (d, *J* = 7.9 Hz, 1H), 7.35 (d, *J* = 8.1 Hz, 1H), 7.30 (s, 1H), 7.08 (t, *J* = 7.5 Hz, 1H), 6.98–6.99 (m, 3H), 6.92–6.90 (m, 1H), 5.77 (s, 1H), 3.85 (s, 2H), 3.73 (s, 3H), 3.65 (s, 3H), 3.51–3.44 (m, 1H), 1.69–1.60 (m, 2H), 1.56–1.50 (m, 3H), 1.23–1.15 (m, 2H), 1.12–0.96 (m, 3H). ^{13}C NMR (125 MHz, DMSO-d_6) δ: 171.1, 167.4, 149.3, 148.9, 136.5, 128.7, 127.5, 124.6 (2C), 121.5, 120.3, 119.1, 118.9, 111.9, 111.8, 111.3, 107.2, 75.4, 55.9, 55.8, 47.9, 32.4, 31.1, 25.5, 24.9, 24.8. Anal. Calcd. For $C_{26}H_{30}N_2O_5$: C, 69.31; H, 6.71; N, 6.22. Found: C, 69.59; H, 6.54; N, 6.42; ESI-MS *m/z*: 450.4 M^+.

4. 3. MTT Assay

A standard MTT assay with an acceptable method was used to determine the *in vitro* cytotoxicity of synthesized indole derivatives.[30] Cancer and normal cell lines (MCF-7, A549, Hela, and MCF-10A) from the Iranian Biological Resource Center, were grown in DMEM Medium with 10% FBS, 1% L glutamine, and 50 mg/mL gentamicin sulfate. Cancer cells were planted into 96-well micro-plates and incubated at 37 °C in a CO_2 incubator overnight (hu-

midified condition of 5% CO_2). Different concentrations of target compounds (in five doses) were prepared by dissolving in DMSO and DMEM Medium. The cells were treated with prepared doses and incubated at 37 ºC for 48 hours. The negative control was untreated cells with 0.1% DMSO and Doxorubicin was used as the positive reference drug. The final concentration of DMSO in all wells, including controls, did not exceed 0.5% (v/v), which was confirmed to be non-toxic to the cells. Then, a fresh medium containing 0.5 mg/mL of MTT was added, and incubation continued for 4 hours. Optical density was measured using an ELISA reader at 540 nm. The IC_{50} values (the concentration required to inhibit cell proliferation by 50%) were determined from the dose-response curves of three independent experiments.[31–33]

4. 4. Analysis of Cellular Apoptosis

HeLa cells, pre-cultured for 16 hours, were seeded at a density of 1×10^5 into six-well plates, and exposed to various concentrations of the target compound for 24 hours. AnnexinV/PI staining was performed using eBioscience TM Annexin V apoptosis detection kit (Invitrogen). After incubation, the cells were trypsinized and washed with phosphate buffered saline (PBS), and 1000 µL 1X binding buffer. Next, the cells were suspended with 100 µL of binding buffer containing 5 µL of Annexin V-fluorescein isothiocyanate (Annexin V-FITC) for 15 minutes. After washing with 1000 µL Binding buffer again, the HeLa cells were resuspended in 200 µL of the same buffer containing 5 µL Propodium Iodide (PI) solution. A BD FACS Calibur™ flow cytometer (BD Biosciences, San Jose, CA, USA) was used to determine the apoptosis percentages as the sum of early and late apoptosis.[34,35]

4. 5. Molecular Docking Studies

Molecular docking studies were performed to investigate possible interactions between the receptor and the ligand using AutoDock 4.2. The structures of Bcl-xL (PDB code: 4C5D, resolution: 2.30) were obtained from the protein databank. A series of changes were applied in the receptor structure to create the corresponding pdbqt file, such as removing benzoylurea as a co-crystallized inhibitor, water molecules, 1,2-ethanediol, and sulfate ion. The structure of synthesized compounds **4a-o** was drawn with hyperchem software and optimized using the semi-empirical PM3 method. Then, the most stable conformation was utilized for docking calculation. The AutoDock 4.2 was used to generate the docking input files. For docking the synthesized compounds into the Bcl-xL structure, Auto Dock 1.5.6 software was used. The size of the grid box was set to 40 × 40 × 40 points with a grid spacing of 0.375 Å. The center of the grid box was set to x = −15.047, y = −25.041, and z = −12.957. For each ligand, 100 independent Lamarckian Genetic Algorithm (LGA) runs were performed. The grid parameters were set according to default parameters, and finally, the files containing the obtained results were analyzed using the Accelrys Discovery Studio Visualizer 3.0 program and the PyMOL Molecular Graphics System.[36]

Declaration of competing interests

The authors declare that they have no known competing financial interests or personal relationships that could have appeared to influence the work reported in this paper.

Acknowledgments

This work was supported by the Ahvaz Jundishapur University of Medical Sciences. A. M. is grateful to the Toxicology Research Center, Medical Basic Sciences Research Institute, Ahvaz Jundishapur University of Medical Sciences, and Central Research Laboratory of Ahvaz Jundishapur University of Medical Sciences. The article was extracted from Project code: TRC-9929 (Ethics: IR.AJUMS.REC.1399.901).

5. References

1. M. F. A. Mohamed, G. E.-D. A. Abuo-Rahma, *RSC Adv.* **2020**, *10*, 31139–31155. **DOI:**10.1039/D0RA05594H
2. H. Sung, J. Ferlay, R. L. Siegel, M. Laversanne, I. Soerjomataram, A. Jemal, F. Bray, *CA Cancer J. Clin.* **2021**, *71,* 209–249. **DOI:**10.3322/caac.21660
3. A. Ayati, S. Moghimi, S. Salarinejad, M. Safavi, B. Pouramiri, A. Foroumadi, *Bioorg. Chem.* **2020**, *99,* 103811. **DOI:**10.1016/j.bioorg.2020.103811
4. A. Ayati, S. Moghimi, M. Toolabi, A. Foroumadi, *Eur. J. Med. Chem.* **2021**, *221,* 113523. **DOI:**10.1016/j.ejmech.2021.113523
5. A. Kumari, R. K. Singh, *Bioorg. Chem.* **2019**, 89, 103021. **DOI:**10.1016/j.bioorg.2019.103021
6. M. Chauhan, A. Saxena, B. Saha, *Eur. J. Med. Chem.* **2021**, *218,* 113400. **DOI:**10.1016/j.ejmech.2021.113400
7. R. G. Panchal, R. L. Ulrich, D. Lane, M. M. Butler, C. Houseweart, T. Opperman, J. D. Williams, N. P. Peet, D. T. Moir, T. Nguyen, R. Gussio, T. Bowlin, S. Bavari, *Antimicrob. Agents Chemother.* **2009**, *53,* 4283–4291. **DOI:**10.1128/AAC.01620-08
8. W. Hong, J. Li, Z. Chang, X. Tan, H. Yang, Y. Ouyang, Y. Yang, S. Kaur, I. C. Paterson, Y. F. Ngeow, H. Wang, *J. Antibiot.* **2017**, *70,* 832–844. **DOI:**10.1038/ja.2017.63
9. B. He, Y. Hu, P. Mao, T. Deng, Y. Wang, X. Luo, H. Zou, Z. Wang, W. Xue, *Arab. J. Chem.* **2024**, *17,* 105758. **DOI:**10.1016/j.arabjc.2024.105758
10. H.-F. Lin, Y.-C. Jiang, Z.-W. Chen, L.-L. Zheng, *RSC Adv.* **2024**, *14,* 16349–16357. **DOI:**10.1039/D4RA00557K
11. H. A. Hamid, A. N. M. Ramli, M. M. Yusoff, *Front. Pharma-*

col. **2017**, *8,* 96. **DOI:**10.3389/fphar.2017.00096
12. C. Tan, S.-J. Yang, D.-H. Zhao, J. Li, L.-Q. Yin, *Arab. J. Chem.* **2022**, *15,* 103756. **DOI:**10.1016/j.arabjc.2022.103756
13. Y. Zhu, J. Zhao, L. Luo, Y. Gao, H. Bao, P. Li, H. Zhang, *Eur. J. Med. Chem.* **2021**, *223*, 113665. **DOI:**10.1016/j.ejmech.2021.113665
14. S. Kumar, Ritika, *Future J. Pharm. Sci.* **2020**, *6,* 121. **DOI:**10.1186/s43094-020-00144-9
15. Y. Wan, Y. Li, C. Yan, M. Yan, Z. Tang, *Eur. J. Med. Chem.* **2019**, *183,* 111691. **DOI:**10.1016/j.ejmech.2019.111691
16. A. Dhiman, R. Sharma, R. K. Singh, *Acta Pharm. Sin. B.* **2022**, *12,* 3006–3027. **DOI:**10.1016/j.apsb.2022.03.021
17. S. Dadashpour, S. Emami, *Eur. J. Med. Chem.* **2018**, *150,* 9–29. **DOI:**10.1016/j.ejmech.2018.02.065
18. A. Gaur, M. N. Peerzada, N. S. Khan, I. Ali, A. Azam, *ACS Omega* **2022**, *7,* 42036–42043. **DOI:**10.1021/acsomega.2c03908
19. S. Dadashpour, S. Emami, *Eur. J. Med. Chem.* **2018**, *150,* 9–29. **DOI:**10.1016/j.ejmech.2018.02.065
20. A. Negi, P. V. Murphy, *Eur. J. Med. Chem.* **2021**, *210,* 113038. **DOI:**10.1016/j.ejmech.2020.113038
21. R. O. Rocha, M. O. Rodrigues, B. A. D. Neto, *ACS Omega* **2020**, *5,* 972–979. **DOI:**10.1021/acsomega.9b03488
22. L. Banfi, A. Basso, C. Lambruschini, L. Moni, R. Riva, *Chem. Sci.* **2021**, *12,* 15445–15472. **DOI:**10.1039/D1SC03810A
23. S. Choi, Z. Chen, L. H. Tang, Y. Fang, S. J. Shin, N. C. Panarelli, Y.-T. Chen, Y. Li, X. Jiang, Y.-C. N. Du, *Nat. Commun.* **2016**, *7,* 10384. **DOI:**10.1038/ncomms10384
24. S. Qian, Z. Wei, W. Yang, J. Huang, Y. Yang, J. Wang, *Front. Oncol.* **2022**, *12,* 985363. **DOI:**10.3389/fonc.2022.985363
25. M. Toolabi, S. Moghimi, T. O. Bakhshaiesh, S. Salarinejad, A. Aghcheli, Z. Hasanvand, E. Nazeri, A. Khalaj, R. Esmaeili, A. Foroumadi, *Eur. J. Med. Chem.* **2020**, *185,* 111786. **DOI:**10.1016/j.ejmech.2019.111786
26. F. Beygi, A. Mostoufi, A. Mojaddami, *Chem. Biodivers.* **2022**, *19,* e202100754. **DOI:**10.1002/cbdv.202100754
27. B. M. F. Gonçalves, V. I. S. Mendes, S. M. Silvestre, J. A. R. Salvador, *RSC Med. Chem.* **2023**, *14,* 313–331. **DOI:**10.1039/D2MD00275B
28. M. Toolabi, F. Safari, A. Ayati, P. Fathi, S. Moghimi, S. Salarinejad, R. Foroumadi, S. H. M. Ketabforoosh, A. Foroumadi, *Arch. Pharm. (Weinheim)* **2022**, *355,* e2100397. **DOI:**10.1002/ardp.202100397
29. B. Zognjani, A. R. Nixha, H. E. Duran, M. Arslan, G. Yıldıztekin, A. Ece, C. Türkeş, *Bioorg. Chem.* **2025**, *163,* 108788. **DOI:**10.1016/j.bioorg.2025.108788
30. S. Gundogdu, H. E. Duran, M. Arslan, B. D. Çetinkaya, C. Türkeş, *Bioorg. Chem.* **2025**, *163,* 108689. **DOI:**10.1016/j.bioorg.2025.108689
31. A. Ayati, R. Esmaeili, S. Moghimi, T. Oghabi Bakhshaiesh, Z. Eslami-S, K. Majidzadeh-A, M. Safavi, S. Emami, A. Foroumadi, *Eur. J. Med. Chem.* **2018**, 145, 404–412. **DOI:**10.1016/j.ejmech.2018.01.015
32. A. Mojaddami, S. Abedanzadeh, M. Bagherzadeh, G. Foroutan, M. J. Khodayar, M. Panahimehr, M. Fereidoonnezhad, *Chem. Biodivers.* **2023**, *20,* e202201177. **DOI:**10.1002/cbdv.202201177
33. Ö. Güleç, H. E. Duran, M. Arslan, G. Yıldıztekin, A. Ece, C. Türkeş, *Bioorg. Chem.* **2025**, *164,* 108861. **DOI:**10.1016/j.bioorg.2025.108861
34. A. Ayati, T. Oghabi Bakhshaiesh, S. Moghimi, R. Esmaeili, K. Majidzadeh-A, M. Safavi, L. Firoozpour, S. Emami, A. Foroumadi, *Eur. J. Med. Chem.* **2018**, *155,* 483–491. **DOI:**10.1016/j.ejmech.2018.06.016
35. A. Mojaddami, A. Karimi, M. Mahdavinia, M. Fereidoonnezhad, *Biometals* **2022**, *35,* 617–627. **DOI:**10.1007/s10534-022-00389-2
36. S. Faeze Mortazavi, A. Ebadi, M. Navid Mohammadian, A. Mojaddami, M. Toolabi, *Chem. Biodivers.* **2025**, *22*, e202402170. **DOI:**10.1002/cbdv.202402170

Povzetek

Sintetizirani so bili novi indolni analogi , in sicer s pomočjo enolončne večkomponentne Passerinijeve reakcije. Nato so avtorji ocenili njihovo protirakavo aktivnosti na celičnih linijah raka HeLa, MCF-7 in A549 z uporabo MTT-testa. Med sintetiziranimi spojinami je (2-(cikloheksilamino)-1-(3-fluorofenil)-2-oksoetil 2-(1H-indol-3-il)acetat (4f) pokazala najmočnejšo citotoksično aktivnost in izkazala obetavne rezultate z IC_{50}-vrednostmi 17,71 in 19,92 μM proti celicam HeLa oziroma MCF-7. Analiza s pretočno citometrijo je potrdila, da spojina 4f pomembno inducira apoptozo v celicah HeLa na koncentracijsko odvisen način. Poleg tega so študije molekulskega sidranja v aktivno mesto antiapoptotskega proteina Bcl-xL pokazale, da se spojina **4f** veže z dobro afiniteto, kar je skladno z njeno znatno učinkovitostjo v *in vitro* testih.